Title: Subgroup-specific structural variation across 1,000 medulloblastoma genomes.

Authors: Northcott PA, Shih DJ, Peacock J, Garzia L, Morrissy AS, Zichner T, Stütz AM, Korshunov A, Reimand J, Schumacher SE, Beroukhim R, Ellison DW, Marshall CR, Lionel AC, Mack S, Dubuc A, Yao Y, Ramaswamy V, Luu B, Rolider A, Cavalli FM, Wang X, Remke M, Wu X, Chiu RY, Chu A, Chuah E, Corbett RD, Hoad GR, Jackman SD, Li Y, Lo A, Mungall KL, Nip KM, Qian JQ, Raymond AG, Thiessen NT, Varhol RJ, Birol I, Moore RA, Mungall AJ, Holt R, Kawauchi D, Roussel MF, Kool M, Jones DT, Witt H, Fernandez-L A, Kenney AM, Wechsler-Reya RJ, Dirks P, Aviv T, Grajkowska WA, Perek-Polnik M, Haberler CC, Delattre O, Reynaud SS, Doz FF, Pernet-Fattet SS, Cho BK, Kim SK, Wang KC, Scheurlen W, Eberhart CG, Fèvre-Montange M, Jouvet A, Pollack IF, Fan X, Muraszko KM, Gillespie GY, Di Rocco C, Massimi L, Michiels EM, Kloosterhof NK, French PJ, Kros JM, Olson JM, Ellenbogen RG,

Published in final edited form as:
Nature. 2012 August 2; 488(7409): 49–56. doi:10.1038/nature11327.

Subgroup specific structural variation across 1,000 medulloblastoma genomes

Paul A Northcott[1,*], **David JH Shih**[1,2,*], **John Peacock**[1,2], **Livia Garzia**[1], **Sorana Morrissy**[1], **Thomas Zichner**[3], **Adrian M Stütz**[3], **Andrey Korshunov**[4], **Juri Reimand**[5], **Steven E Schumacher**[6], **Rameen Beroukhim**[6,7,8,9,10,11], **David W Ellison**[12], **Christian R Marshall**[13], **Anath C Lionel**[14], **Stephen Mack**[1,2], **Adrian Dubuc**[1,2], **Yuan Yao**[1,2], **Vijay Ramaswamy**[1,2], **Betty Luu**[1], **Adi Rolider**[1], **Florence Cavalli**[1], **Xin Wang**[1,2], **Marc Remke**[1], **Xiaochong Wu**[1], **Readman YB Chiu**[15], **Andy Chu**[15], **Eric Chuah**[15], **Richard D Corbett**[15], **Gemma R Hoad**[15], **Shaun D Jackman**[15], **Yisu Li**[15], **Allan Lo**[15], **Karen L Mungall**[15], **Ka Ming Nip**[15], **Jenny Q Qian**[15], **Anthony GJ Raymond**[15], **Nina Thiessen**[15], **Richard J Varhol**[15], **Inanc Birol**[15], **Richard A Moore**[15], **Andrew J Mungall**[15], **Robert Holt**[16], **Daisuke Kawauchi**[17], **Martine F Roussel**[17], **Marcel Kool**[18], **David TW Jones**[18], **Hendrick Witt**[19,20], **Africa Fernandez-L**[21], **Anna M Kenney**[22,23], **Robert J Wechsler-Reya**[24], **Peter Dirks**[25], **Tzvi Aviv**[26], **Wieslawa A Grajkowska**[27], **Marta Perek-Polnik**[28], **Christine C Haberler**[29], **Olivier Delattre**[30], **Stéphanie S Reynaud**[31], **François F Doz**[32], **Sarah S Pernet-Fattet**[33], **Byung-Kyu Cho**[34], **Seung-Ki Kim**[34], **Kyu-Chang Wang**[34], **Wolfram Scheurlen**[35], **Charles G Eberhart**[36], **Michelle Fèvre-Montange**[37], **Anne Jouvet**[38], **Ian F Pollack**[39], **Xing Fan**[40], **Karin M Muraszko**[41], **G. Yancey Gillespie**[42], **Concezio Di Rocco**[43], **Luca Massimi**[43], **Erna MC Michiels**[44], **Nanne K Kloosterhof**[44,45], **Pim J French**[45], **Johan M Kros**[46], **James M Olson**[47,48], **Richard G**

Correspondence and requests for materials should be addressed to MAM (mmarra@bcgsc.ca) and MDT (mdtaylor@sickkids.ca).
[*]These authors contributed equally
[#]These authors contributed equally

Author Contributions

PAN and MDT co-conceived the study. PAN, MAM, and MDT led the study. PAN planned and executed experiments and analyses, supervised data acquisition, performed bioinformatic analyses, and extracted nucleic acids for the MAGIC cohort. DJHS led the bioinformatics and performed analyses. JP performed quantitative RT-PCR and Sanger sequencing of PVT1 fusions, expression profiled PVT1-encoded miRNAs, and generated schematics for PVT1 fusion genes. LG performed the MYC and miR-1204 knockdown experiments. SM supervised the RNASeq and WGS experiments and performed data analysis. TZ, AMS, and JOK performed the large insert paired-end sequencing and PCR verification of SNCAIP duplication samples. AK performed interphase FISH and IHC for candidate genes. JR and GBD led the pathway analyses and generated enrichment plots. SES and RB provided technical support with the GISTIC2 bioinformatic platform. DWE performed interphase FISH for candidate genes. CRW, ACL, and SWS performed the SNP6 genotyping analysis, provided a database of normal copy number variants, and the control dataset used to infer copy number in the tumour samples. SM, AD, FC, MK, DTWJ, and HW performed bioinformatic analyses and provided technical advice. YY sequenced *CTNNB1* in the WNT tumours. VR, DK, MFR, TA, and PD performed functional assays for candidate genes. BL extracted nucleic acids, managed biobanking, and maintained the patient database. SM and AR performed the drug database analysis. Xin W, Xiaochong W, and MR provided technical support. RYBC, AC, EC, RDC, GRH, SDJ, YL, AL, KLM, KMN, JQQ, AGJR, NT, RJV, IB, RAM, AJM, RH, and SJMJ led the RNASeq and WGS experiments and performed data analyses. AFL and AMK provided the database of Shh-responsive genes. RJWR, WAG, MPP, CCH, OD, SSR, FFD, SSPF, BKC, SKK, KCW, WS, CGE, MFM, AJ, IFP, XF, KMM, GYG, CDR, LM, EMCM, NKN, PJF, JMK, JMO, RGE, KZ, LK, RCT, MKC, BL, REM, DDB, AF, SA, NJ, JCL, SB, NG, WAW, LB, AK, TEVM, TK, TT, SKE, JRL, JBR, LML, EGVM, MF, HN, GC, MG, PH, AGS, AI, SJ, CGC, RV, YSR, SR, MZ, CCF, JAC, MLL, YJC, UT, CEH, EB, SCC, and SMP provided the patient samples and clinical details that made the study possible. PHBS, MM, SLP, YJC, UT, CEH, EB, SWS, JTR, DM, SCC, SJMJ, JOK, SMP, and MAM provided valuable input regarding study design, data analysis, and interpretation of results. PAN, DJHS, JP, LG, SM, and MDT wrote the manuscript. MAM and MDT provided financial and technical infrastructure and oversaw the study. MAM and MDT are joint senior authors and project co-leaders.

Author information

SNP6 copy number and gene expression array data have been deposited at the Gene Expression Omnibus (GEO; http://www.ncbi.nlm.nih.gov/geo/) as a GEO SuperSeries under accession number GSE37385. Whole genome and transcriptome sequencing data have been deposited at the European Genome-phenome Archive (EGA; https://www.ebi.ac.uk/ega/) hosted by the EBI, under accession number EGAD00001000158.

The authors declare no competing financial interests.

Ellenbogen[49], **Karel Zitterbart**[50,51], **Leos Kren**[52], **Reid C Thompson**[22], **Michael K Cooper**[53], **Boleslaw Lach**[54,55], **Roger E McLendon**[56], **Darell D Bigner**[56], **Adam Fontebasso**[57], **Steffen Albrecht**[58,59], **Nada Jabado**[57,60], **Janet C Lindsey**[61], **Simon Bailey**[61], **Nalin Gupta**[62], **William A Weiss**[63], **László Bognár**[64], **Almos Klekner**[64], **Timothy E Van Meter**[65], **Toshihiro Kumabe**[66], **Teiji Tominaga**[66], **Samer K Elbabaa**[67], **Jeffrey R Leonard**[68], **Joshua B Rubin**[69], **Linda M Liau**[70], **Erwin G Van Meir**[71], **Maryam Fouladi**[72], **Hideo Nakamura**[73], **Giuseppe Cinalli**[74], **Miklós Garami**[75], **Peter Hauser**[75], **Ali G Saad**[76], **Achille Iolascon**[77,78], **Shin Jung**[79], **Carlos G Carlotti**[80], **Rajeev Vibhakar**[81], **Young Shin Ra**[82], **Shenandoah Robinson**[83,84], **Massimo Zollo**[77,78], **Claudia C Faria**[85,86], **Jennifer A Chan**[87], **Michael L Levy**[88], **Poul HB Sorensen**[89], **Matthew Meyerson**[7], **Scott L Pomeroy**[90], **Yoon-Jae Cho**[91], **Gary D Bader**[5,13,92,93], **Uri Tabori**[94], **Cynthia E Hawkins**[95], **Eric Bouffet**[94], **Stephen W Scherer**[13,14], **James T Rutka**[25], **David Malkin**[94,96], **Steven C Clifford**[61], **Steven JM Jones**[15], **Jan O Korbel**[3], **Stefan M Pfister**[18,19], **Marco A Marra**[16,97,#], and **Michael D Taylor**[1,2,25,#]

[1]Developmental & Stem Cell Biology Program, The Hospital for Sick Children, 101 College Street, TMDT-11-401M, Toronto, Ontario, Canada, M5G 1L7 [2]Department of Laboratory Medicine and Pathobiology, University of Toronto, Medical Sciences Buildings, 1 King's College Circle, 6th Floor, Toronto, Ontario, Canada, M5S 1A8 [3]Genome Biology, European Molecular Biology Laboratory, Meyerhofstr. 1, Heidelberg, Germany, 69117 [4]CCU Neuropathology, German Cancer Research Center (DKFZ), Im Neuenheimer Feld 220-221, Department of Neuropathology, University of Heidelberg, Im Neuenheimer Feld 224, Heidelberg, Germany, 69120 [5]The Donnelly Centre, University of Toronto, 160 College Street, Room 602, Toronto, Ontario, Canada, M5S 3E1 [6]Department of Cancer Biology, Dana-Farber Cancer Institute, 450 Brookline Avenue, Boston, Maine, United States, 02215 [7]Department of Medical Oncology, Dana-Farber Cancer Institute, 450 Brookline Avenue, Boston, Maine, United States, 02215 [8]Department of Medicine, Harvard Medical School, 25 Shattuck Street, Boston, Maine, United States, 02115 [9]Department of Medicine, Brigham and Women's Hospital, 75 Francis St, Boston, Maine, United States, 02115 [10]Cancer Program, Broad Institute, 7 Cambridge Center, Cambridge, Maine, United States, 02142 [11]Center for Cancer Genome Discovery, Dana-Farber Cancer Institute, 450 Brookline Avenue, Boston, Maine, United States, 02215 [12]Pathology, St. Jude Children's Research Hospital, 262 Danny Thomas Place, Memphis, Tennessee, United States, 38105 [13]McLaughlin Centre and Department of Molecular Genetics, University of Toronto, 101 College Street, Toronto, Ontario, Canada, M5G 1L7 [14]The Centre for Applied Genomics and Program in Genetics and Genome Biology, The Hospital for Sick Children, 101 College Street, TMDT-14-701, Toronto, Ontario, Canada, M5G 1L7 [15]Michael Smith Genome Sciences Centre, BC Cancer Agency, 100-570 West 7th Avenue, Vancouver, British Columbia, Canada, V5Z 4S6 [16]Michael Smith Genome Sciences Centre, BC Cancer Agency, 675 West 10th Avenue, Vancouver, British Columbia, Canada, V5Z 1L3 [17]Tumour Cell Biology, St. Jude Children's Research Hospital, 262 Danny Thomas Place, Memphis, Tennessee, United States, 38105 [18]Division of Pediatric Neurooncology, German Cancer Research Center (DKFZ), Im Neuenheimer Feld 280, Heidelberg, Germany, 69120 [19]Department of Pediatric Oncology, University Hospital Heidelberg, Im Neuenheimer Feld 430, Heidelberg, Germany, 69120 [20]Departments of Hematology and Immunology, University Hospital Heidelberg, Im Neuenheimer Feld 430, Heidelberg, Germany, 69120 [21]Pediatric Clinical Trials Office, Memorial Sloan-Kettering Cancer Center, 405 Lexington Avenue, New York, New York, United States, 10174 [22]Neurological Surgery, Vanderbilt Medical Center, T-4224 MCN, Nashville, Tennessee, United States, 37232-2380 [23]Cancer Biology, Vanderbilt Medical Center, 465 21st Avenue South, MRB III 6160, Nashville, Tennessee, United States, 37232-8550 [24]Sanford-Burnham Medical Research Institute, La Jolla, California, United States, 92037 [25]Department of Surgery, Division of Neurosurgery and Labatt Brain Tumour Research Centre, The Hospital for Sick Children, 555 University Avenue, Hill 1503, Toronto, Ontario, Canada, M5G 1X8 [26]Developmental & Stem Cell Biology Program, The Hospital for Sick Children, 101 College Street, TMDT-13-601, Toronto,

Ontario, Canada, M5G 1L7 [27]Department of Pathology, The Children's Memorial Health Institute, Aleja Dzieci Polskich20, Warsaw, Poland, 04-730 [28]Department of Oncology, The Children's Memorial Health Institute, Aleja Dzieci Polskich20, Warsaw, Poland, 04-730 [29]Institute of Neurology, Medical University of Vienna, AKH 4J, Waehringer Gürtel 18-20, A-1097, Vienna, Austria [30]INSERM U 830, Institut Curie, 26 rue D'Ulm, Paris Cedex 5, France, 75238 [31]Unit of Somatic Genetics, Institut Curie, 26 rue d'Ulm, Paris Cedex 5, France, 75238 [32]Department of Pediatric Oncology, Institut Curie, 26 rue D'Ulm, Paris Cedex 5, France, 75248 [33]Pediatric Hematology and Oncology, CHUV University Hospital, Lausanne, Switzerland [34]Department of Neurosurgery, Division of Pediatric Neurosurgery, Seoul National University Children's Hospital, 101 Daehak-Ro Jongno-Gu, Seoul, Korea, 110-744 [35]Head of Pediatrics, Cnopf´sche Kinderklinik, Theodor-Kutzer-Ufer 1-3, Nuremberg, Germany [36]Departments of Pathology, Ophthalmology and Oncology, John Hopkins University School of Medicine, 720 Rutland Avenue, Ross Building 558, Baltimore, Maryland, United States, 21205 [37]INSERM U1028, CNRS UMR5292, Centre de Recherche en Neurosciences, Université de Lyon, Lyon, France [38]Centre de Pathologie EST, Groupement Hospitalier EST, Université de Lyon, Bron, France [39]Department of Neurological Surgery, University of Pittsburgh School of Medicine, 4401 Penn Avenue, Pittsburgh, Pennsylvania, United States, 15224 [40]Departments of Neurosurgery and Cell and Developmental Biology, University of Michigan Medical School, 109 Zina Pitcher Place, 5018 BSRB, Ann Arbor, Michigan, United States, 48109 [41]Department of Neurosurgery, University of Michigan Medical School, 1500 E. Medical Center Drive, Taubman Center, Room 3552, Ann Arbor, Michigan, United States, 48109 [42]Department of Surgery, Division of Neurosurgery, University of Alabama at Birmingham, 1900 University Boulevard, THT 1052, Birmingham, Alabama, United States, 35294-0006 [43]Pediatric Neurosurgery, Catholic University Medical School, Rome, Italy [44]Department of Pediatric Oncology and Hematology, Erasmus Medical Center, Dr. Molewaterplein 50, Rotterdam, Netherlands [45]Department of Neurology, Erasmus Medical Center, Dr. Molewaterplein 50, PO Box 2040, 3000 CA, Rotterdam, Netherlands [46]Department of Pathology, Erasmus Medical Center, Dr. Molewaterplein 50, 3015 GE, Rotterdam, Netherlands [47]Clinical Research Division, Fred Hutchinson Cancer Research Center, 1100 Fairview Avenue North, D4-100, Seattle, Washington, United States [48]Seattle Children's Hospital, Seattle, Washington, United States [49]Neurological Surgery, University of Washington School of Medicine, Harborview Medical Center, 325 Ninth Avenue, Seattle, Washington, United States, 98104 [50]Department of Pediatric Oncology, School of Medicine, Masaryk University, Cernopolni 9, 613 00, Brno, Czech Republic [51]Department of Pediatric Oncology, University Hospital Brno, Brno, Czech Republic [52]Department of Pathology, University Hospital Brno, Jihlavska 20, 625 00, Brno, Czech Republic [53]Department of Neurology, Vanderbilt Medical Center, 465 21st Avenue South, MRB III 6160, Nashville, Tennessee, United States, 37232-8550 [54]Department of Pathology and Molecular Medicine, Division of Anatomical Pathology, McMaster University, Hamilton, Ontario, Canada [55]Department of Pathology and Laboratory Medicine, Hamilton General Hospital, 237 Barton Street East, Hamilton, Ontario, Canada, L8L 2X2 [56]Department of Pathology, Duke University, DUMC 3712, Durham, North Carolina, United States, 27710 [57]Division of Experimental Medicine, McGill University, 4060 Ste Catherine West, Montreal, Quebec, Canada, H3Z 2Z3 [58]Department of Pathology, McGill University, Montreal, Quebec, Canada [59]Department of Pathology, Montreal Children's Hospital, 2300 Tupper, Montreal, Quebec, Canada, H3H 1P3 [60]Department of Pediatrics, Division of Hemato-Oncology, McGill University, Montreal, Quebec, Canada [61]Northern Institute for Cancer Research, Newcastle University, Newcastle upon Tyne, United Kingdom, NE1 4LP [62]Departments of Neurological Surgery and Pediatrics, University of California San Francisco, 505 Parnassus Avenue, Room M779, San Francisco, California, United States, 94143-0112 [63]Departments of Neurology, Pediatrics, and Neurosurgery, University of California San Francisco, The Helen Diller Family Cancer Research Building 1450 3rd Street, Room HD-220, MC 0520, San Francisco, California, United States, 94158 [64]Department of Neurosurgery, University of Debrecen, Medical

and Health Science Centre, Móricz Zs. Krt. 22., Debrecen, Hungary, 4032 [65]Pediatrics, Virginia Commonwealthy University, School of Medicine, Box 980646, Pediatric Hematology-Oncology, 1101 East Marshall Street, Richmond, Virginia, United States, 23298-0646 [66]Department of Neurosurgery, Tohoku University Graduate School of Medicine, 1-1 Seiryo-machi, Aoba-ku, Sendai, Japan, 980-8574 [67]Department of Neurosurgery, Division of Pediatric Neurosurgery, Saint Louis University School of Medicine, 1465 South Grand Boulevard, Suite 3707, Saint Louis, Missouri, United States, 63104 [68]Department of Neurosurgery, Division of Pediatric Neurosurgery, Washington University School of Medicine and St. Louis Children's Hospital, Campus Box 8057, 660 South Euclid Avenue, St. Louis, Missouri, United States, 63110 [69]Departments of Pediatrics, Anatomy and Neurobiology, Washington University School of Medicine and St. Louis Children's Hospital, Campus Box 8208, 660 South Euclid Avenue, St. Louis, Missouri, United States, 63110 [70]Department of Neurosurgery, David Geffen School of Medicine at UCLA, 10833 Le Conte Avenue, Campus 690118, Los Angeles, California, United States, 90095 [71]Departments of Neurosurgery and Hematology & Medical Oncology, School of Medicine and Winship Cancer Institute, Emory University, 1365C Clifton Road NE, 57 Laboratory of Molecular Neuro-Oncology, Atlanta, Georgia, United States, 30322 [72]Division of Oncology, University of Cincinnati, Cincinnati Children's Hospital Medical Center, Cincinnati, Ohio, United States [73]Department of Neurosurgery, Kumamoto University Graduate School of Medical Science, 1-1-1, Honjo, Kumamoto, Japan, 860-8556 [74]Paediatric Neurosurgery, Ospedale Santobono-Pausilipon, Naples, Italy [75]2nd Department of Pediatrics, Semmelweis University, Budapest, Hungary [76]Pathology, University of Arkansas for Medical Sciences, 1 Children's Way, lot # 820, Little Rock, Arkansas, United States, 72202 [77]Dipartimento di Biochimica e Biotecnologie Mediche, University of Naples, Via Pansini 5, Naples, Italy [78]CEINGE Biotecnologie Avanzate, Via Gaetano Salvatore 486, 80145, Naples, Italy [79]Department of Neurosurgery, Chonnam National University Research Institute of Medical Sciences, Chonnam National University Hwasun Hospital and Medical School, 322 Seoyang-ro, Hwasun-eup, Hwasun-gun, Chonnam, South Korea, 519-763 [80]Department of Surgery and Anatomy, Faculty of Medicine of Ribeirão Preto, Universidade de São Paulo, Brazil, Avenida Bandeirantes, 3900, Monte Alegre, Rebeirao Preto, São Paulo, Brazil [81]Pediatrics, University of Colorado Denver, 12800 19th Avenue, Aurora, Colorado, United States, 80045 [82]Department of Neurosurgery, University of Ulsan, Asan Medical Center, Seoul, Korea [83]Division of Pediatric Neurosurgery, Case Western Reserve, Cleveland, Ohio, United States [84]Rainbow Babies & Children's, Cleveland, Ohio, United States [85]Division of Neurosurgery, Hospital de Santa Maria, Centro Hospitalar Lisboa Norte EPE, Lisbon, Portugal [86]Cell Biology Program, The Hospital for Sick Children, 101 College Street, TMDT-401-J, Toronto, Ontario, Canada, M5G 1L7 [87]Department of Pathology and Laboratory Medicine, University of Calgary, 3330 Hospital Drive NW, HRIC 2A25A, Calgary, Alberta, Canada, T2N 4N1 [88]UCSD Division of Neurosurgery, Rady Children's Hospital San Diego, 8010 Frost Street, Suite 502, San Diego, California, United States [89]Department of Molecular Oncology, British Columbia Cancer Research Centre, 675 West 10th Avenue, Vancouver, British Columbia, Canada, V5Z 1L3 [90]Department of Neurology, Harvard Medical School, Children's Hospital Boston, Fegan 11, 300 Longwood Avenue, Boston, Maine, United States, 02115 [91]Department of Neurology and Neurological Sciences, Stanford University School of Medicine, 1201 Welch Road, MSLS Building, Rm P213, Stanford, California, United States, 94305 [92]Banting and Best Department of Medical Research, University of Toronto, Toronto, Ontario, Canada [93]Samuel Lunenfeld Research Institute at Mount Sinai Hospital, University of Toronto, Toronto, Ontario, Canada [94]Department of Haematology & Oncology, The Hospital for Sick Children, 555 University Avenue, Toronto, Ontario, Canada, M5G 1X8 [95]Department of Pathology, The Hospital for Sick Children, 555 University Avenue, Toronto, Ontario, Canada, M5G 1X8 [96]Department of Pediatrics, University of Toronto, Toronto, Ontario, Canada [97]Department of Medical Genetics, University of British Columbia, 675 West 10th Avenue, Vancouver, British Columbia, Canada, V5Z 1L3

Summary

Medulloblastoma, the most common malignant pediatric brain tumour, is currently treated with non-specific cytotoxic therapies including surgery, whole brain radiation, and aggressive chemotherapy. As medulloblastoma exhibits marked intertumoural heterogeneity, with at least four distinct molecular variants, prior attempts to identify targets for therapy have been underpowered due to small samples sizes. Here we report somatic copy number aberrations (SCNAs) in 1087 unique medulloblastomas. SCNAs are common in medulloblastoma, and are predominantly subgroup enriched. The most common region of focal copy number gain is a tandem duplication of the Parkinson's disease gene *SNCAIP*, which is exquisitely restricted to Group 4α. Recurrent translocations of *PVT1*, including *PVT1-MYC* and *PVT1-NDRG1* that arise through chromothripsis are restricted to Group 3. Numerous targetable SCNAs, including recurrent events targeting TGFβ signaling in Group 3, and NF-κB signaling in Group 4 suggest future avenues for rational, targeted therapy.

Brain tumours are the most common cause of childhood oncological death, and medulloblastoma is the most common malignant pediatric brain tumour. Current medulloblastoma therapy including surgical resection, whole brain and spinal cord radiation, and aggressive chemotherapy supplemented by bone marrow transplant yields five-year survival rates of 60–70%[1]. Survivors are often left with significant neurological, intellectual, and physical disabilities secondary to the effects of these non-specific cytotoxic therapies on the developing brain[2].

Recent evidence suggests that medulloblastoma actually comprises multiple molecularly distinct entities whose clinical and genetic differences may require separate therapeutic strategies[3–6]. Four principal subgroups of medulloblastoma have been identified: WNT, SHH, Group 3, and Group 4[7], and there is preliminary evidence for clinically significant subdivisions of the subgroups[3,7,8]. Rational, targeted therapies based on genetics are not currently in use for medulloblastoma, although inhibitors of the Sonic Hedgehog pathway protein Smoothened have shown early promise[9]. Actionable targets for WNT, Group 3, and Group 4 tumours have not been identified[4,10]. Sanger sequencing of 22 medulloblastoma exomes revealed on average only 8 SNVs per tumour[11]. Some SNVs were subgroup restricted (*PTCH1*, *CTNNB1*), while others occurred across subgroups (*TP53*, *MLL2*). We hypothesized that the observed intertumoural heterogeneity might have underpowered prior attempts to discover targets for rational therapy.

The Medulloblastoma Advanced Genomics International Consortium (MAGIC) consisting of scientists and physicians from 46 cities across the globe gathered >1200 medulloblastomas which were studied by SNP arrays (n=1239; Figure 1a; Supplementary Figure 1; Supplementary Tables 1–3). Medulloblastoma subgroup affiliation of 827 cases was determined using a custom nanoString-based RNA assay (Supplementary Figure 2)[12]. Disparate patterns of broad cytogenetic gain and loss were observed across the subgroups (Figure 1b; Supplementary Figures 3, 7, 8, 10, 11). Analysis of the entire cohort using GISTIC2[13] to discover significant 'driver' events delineated 62 regions of recurrent SCNA (Figure 1c; Supplementary Figure 4; Supplementary Tables 4–5); analysis by subgroup increased sensitivity such that 110 candidate 'driver' SCNAs were identified, most of which are subgroup enriched (Figure 1c–e; Supplementary Table 6).

Twenty-eight regions of recurrent high-level amplification (copy number ≥5) were identified (Figure 1d; Supplementary Table 7). The most prevalent amplifications affected members of the MYC family with *MYCN* predominantly amplified in SHH and Group 4, *MYC* in Group 3, and *MYCL1* in SHH medulloblastomas. Multiple genes/regions were exclusively amplified in SHH, including *GLI2*, *MYCL1*, *PPM1D*, *YAP1*, and *MDM4* (Figure 1d).

Recurrent homozygous deletions were exceedingly rare, with only 15 detected across 1087 tumours (Figure 1e). Homozygous deletions targeting known tumour suppressors *PTEN*, *PTCH1*, and *CDKN2A/B* were the most common, all enriched in SHH cases (Figure 1e; Supplementary Table 7). Novel homozygous deletions included *KDM6A*, a histone-lysine demethylase deleted in Group 4. A custom nanoString CodeSet was used to verify 24 significant regions of gain across 192 MAGIC cases, resulting in a verification rate of 90.9% (Supplementary Figure 5). We conclude that SCNAs in medulloblastoma are common, and are predominantly subgroup enriched.

Subgroup-specific SCNAs in medulloblastoma

WNT medulloblastoma genomes are impoverished of recurrent focal regions of SCNA, exhibiting no significant regions of deletion and only a small subset of focal gains found at comparable frequencies in non-WNT tumours (Supplementary Figures 4, 6; Supplementary Table 8). *CTNNB1* mutational screening confirmed canonical exon 3 mutations in 63/71 (88.7%) WNT tumours, whereas monosomy 6 was detected in 58/76 (76.3%) (Supplementary Figure 6; Supplementary Table 9). Four WNT tumours (4/71; 5.6%) had neither *CTNNB1* mutation nor monosomy 6, but maintained typical WNT expression signatures. Given the size of our cohort and the resolution of the platform, we conclude that there are no frequent, targetable SCNAs for WNT medulloblastoma.

SHH tumours exhibit multiple significant focal SCNAs (Figure 2a; Supplementary Figures 12, 15, 16; Supplementary Tables 10–11). SHH enriched/restricted SCNAs included amplification of *GLI2* and deletion of *PTCH1* (Figure 2a, e, f)[10]. *MYCN* and *CCND2* were among the most frequently amplified genes in SHH (Supplementary Table 6), but were also altered in non-SHH cases. Genes up-regulated in SHH tumours (i.e. SHH signature genes) are significantly over-represented among the genes focally amplified in SHH tumours (P=0.001–0.02, permutation tests; Supplementary Figure 9). Recurrent amplification of SHH signature genes has clinical implications, as amplification of downstream transcriptional targets could mediate resistance to upstream SHH pathway inhibitors[14].

Novel, SHH-enriched SCNAs included components of TP53 signaling, including amplifications of *MDM4* and *PPM1D*, and focal deletions of *TP53* (Figure 2a–e). Targetable events, including amplifications of IGF signaling genes *IGF1R* and *IRS2*, PI3K genes *PIK3C2G* and *PIK3C2B*, and deletion of *PTEN* were restricted to SHH tumours (Figure 2a, c, e). Importantly, focal events affecting genes in the SHH pathway were largely mutually exclusive and prognostically significant (Figure 2f, g). Many of the recurrent, targetable SCNAs identified in SHH medulloblastoma (*IGF1R*, *KIT*, *MDM4*, *PDGFRA*, *PIK3C2G*, *PIK2C2B*, and *PTEN*) have already been targeted with small molecules for treatment of other malignancies, which might allow rapid translation for targeted therapy of subsets of SHH patients (Supplementary Table 16). Novel SHH targets identified here are excellent candidates for combinatorial therapy with Smoothened inhibitors, in order to avoid the resistance encountered in both humans and mice[9,14,15].

Group 3 and Group 4 medulloblastomas have generic names as comparatively little is known about their genetic basis, and no targets for rational therapy have been identified[7]. *MYC* amplicons are largely restricted to Group 3, while *MYCN* amplicons are seen in Group 4 and SHH tumours (Figure 1d)[3,4]. Indeed, *MYC* and *MYCN* loci comprise the most significant regions of amplification observed in Group 3 and Group 4, respectively (Figure 3a, b; Supplementary Figures 13, 14, 17–20; Supplementary Tables 12–15). Group 3 *MYC* amplicons were mutually exclusive from those affecting the known medulloblastoma oncogene *OTX2*[16] and were highly prognostic (Supplementary Figure 21)[3,16]. Type II activin receptors, *ACVR2A* and *ACVR2B* and family member *TGFBR1* are highly

amplified in Group 3 tumours, suggesting deregulation of TGFβ signaling as a driver event in Group 3 (Figure 3c–e; Supplementary Figure 22). The Group 3-enriched medulloblastoma oncogene *OTX2* is a prominent target of TGFβ signaling in the developing nervous system[17] and TGFβ pathway inhibitors, *CD109*[18], *FKBP1A*[19,20], and *SNX6*[20] are recurrently deleted in Group 3 (Figure 3a, d). SCNAs in TGFβ pathway genes were heavily enriched in Group 3 (P=5.37E-05, Fisher's exact test) and found in at least 20.2% of cases, suggesting that TGFβ signaling represents the first rational target for this poor prognosis subgroup (Figure 3d). Similarly, novel deletions affecting regulators of the NF-κB pathway, including *NFKBIA*[21] and *USP4*[22] were identified in Group 4 (Supplementary Figure 23), proposing that NF-κB signaling may represent a rational Group 4 therapeutic target.

Network analysis of Group 3 and Group 4 SCNAs illustrates the different pathways over-represented in each subgroup. Only TGFβ signaling is unique to Group 3 (Figure 3e). In contrast, cell cycle control, chromatin modification, and neuronal development are all Group 4-enriched. Cumulatively, the dismal prognosis of Group 3 patients, the lack of published targets for rationale therapy, and the prior targeting of TGFβ signaling in other diseases suggest that TGFβ may represent an appealing target for Group 3 rational therapies (Supplementary Table 16).

SNCAIP tandem duplication is common in Group 4

Although Group 4 is the most prevalent medulloblastoma subgroup its pathogenesis remains poorly understood. The most frequent SCNA observed in Group 4 (33/317; 10.4%) is a recurrent region of single copy gain on chr5q23.2 targeting a single gene – *SNCAIP* (synuclein, alpha interacting protein) (Figure 4a; Supplementary Figure 24). *SNCAIP*, encodes SYNPHILIN-1, which binds to α-SYNUCLEIN to promote the formation of Lewy bodies in the brains of patients with Parkinson's disease[23,24]. Additionally, rare germline mutations of *SNCAIP* have been described in Parkinson's families[25]. Large insert, mate-pair, whole genome sequencing (WGS) demonstrates that *SNCAIP* copy number gains arise from tandem duplication of a truncated *SNCAIP* (lacking non-coding exon 1), inserted telomeric to the germline *SNCAIP* allele (Figure 4b, c; Supplementary Figure 25). SNP6 profiling of patient-matched germline material confirmed that *SNCAIP* duplications are somatic (Supplementary Figure 26) and subsequent whole transcriptome sequencing (RNASeq) of select Group 4 cases (n=5) verified that SNCAIP is the only gene expressed in the duplicated region (Supplementary Figure 27). Analysis of published copy number profiles for 3131 primary tumours[26] and 947 cancer cell lines[27] (total of 4078 cases) revealed only four cases with apparent duplication of *SNCAIP*, all of which were inferred as Group 4 medulloblastomas (data not shown). We conclude that *SNCAIP* duplication is a somatic event highly specific to Group 4 medulloblastoma.

Re-analysis of 499 published medulloblastoma expression profiles confirmed that SNCAIP is one of the most highly up-regulated Group 4 signature genes (Figure 4d; Supplementary Figure 28). Profiling of 188 Group 4 tumours on expression microarrays followed by consensus non-negative matrix factorization (NMF) clustering delineates two subtypes of Group 4 (4α and 4β; Figure 4e; Supplementary Figure 29). Strikingly, 21/22 *SNCAIP* duplicated cases belonged to Group 4α (P=3.12E-08, Fisher's exact test). SNCAIP is more highly expressed in Group 4α than 4β (Figure 4f), and 4α samples with tandem duplication showed ~1.5-fold increased expression, consistent with gene dosage (Figure 4g; Supplementary Figures 35, 36). Group 4α exhibits a relatively balanced genome compared to 4β (Supplementary Figures 30–32), and several 4α cases harbour *SNCAIP* duplication in conjunction with i17q and no other SCNAs (Supplementary Figure 33). Importantly, SNCAIP duplications are mutually exclusive from other prominent SCNAs in Group 4, including *MYCN* and *CDK6* amplifications (Supplementary Figure 34).

PVT1 fusions arise via chromothripsis in Group 3

Although recurrent gene fusions have recently been discovered in solid tumours, none have been reported in medulloblastoma. RNASeq of Group 3 tumours (n=13) identified two independent gene fusions in two different tumours (MB-182 and MB-586, both involving the 5' end of PVT1 - a non-coding gene frequently co-amplified with *MYC* in Group 3 (Figure 5a, b; Supplementary Figure 37; Supplementary Tables 17–18). Sanger sequencing confirmed a fusion transcript consisting of exons 1 and 3 of PVT1 fused to the coding sequence of MYC (exons 2 & 3) in MB-182, and a fusion involving PVT1 exon 1 fused to the 3' end of NDRG1 in MB-586 (Figure 5a, b).

Group 3 copy number data at the *MYC*/*PVT1* locus suggested that additional samples might harbour PVT1 gene fusions (Figure 5c). RT-PCR profiling of select Group 3 cases confirmed PVT1-MYC fusions in at least 60% (12/20) *MYC*-amplified cases (Figure 5d; Supplementary Table 19). Fusion transcripts included many other portions of chr8q, with up to four different genomic loci mapping to a single transcript, a pattern reminiscent of chromothripsis[28,29] (Figure 5d). WGS performed on four *MYC*-amplified Group 3s harbouring PVT1 fusion transcripts identified a series of complex genomic rearrangements on chr8q (Figure 5e, f; Supplementary Figure 38; Supplementary Tables 20–21). Chromosome 8 copy number profile for MB-586 (*PVT1-NDRG1*) derived from WGS showed that *PVT1* and *NDRG1* are structurally linked as predicted by RNASeq, and several adjacent regions of 8q24 were extensively rearranged (Figure 5e, f; Supplementary Table 21). Monte Carlo simulation suggests that this fragmented 8q amplicon arose through chromothripsis, a process of erroneous DNA repair following a single catastrophic event in which a chromosome is shattered into many pieces (Supplementary Figure 39). Further examination of our copy number dataset revealed rare examples of chromothripsis across subgroups (Supplementary Figure 40), with only chr8 in Group 3 demonstrating statistically significant, region-specific chromothripsis (q=0.0004, FDR-corrected Fisher's exact test). Among Group 3 tumours, the occurrence of chr8q chromothripsis is correlated with deletion of chr17p (location of *TP53*; data not shown), in keeping with the association of loss of TP53 and chromothripsis recently described in medulloblastoma (P=0.0199, Fisher's exact test)[28]. While the *PVT1* locus has been suggested to be a genomically fragile site, we observe that the majority of *MYC*-amplified Group 3 tumours harbour PVT1 fusions that arise through a process consistent with chromothripsis.

PVT1 is a non-coding host gene for 4 miRNAs – miR-1204–1207. Previous studies have implicated miR-1204 as a candidate oncogene that enhances oncogenesis in combination with MYC[30,31]. PVT1 fusions identified in this study involve only PVT1 exon 1 and miR-1204. Importantly, miR-1204, but not the adjacent miR-1205 and miR-1206, is expressed at a higher level in PVT1-MYC fusion(+) Group 3 tumours compared to fusion(−) cases (P=0.0008, Mann-Whitney test; Figure 6a). To evaluate whether aberrant expression of miR-1204 contributes to the malignant phenotype, we inhibited miR-1204 in MED8A cells, a Group 3 medulloblastoma cell line with a confirmed PVT1-MYC fusion (Figure 5d). Antagomir-mediated RNAi of miR-1204 had a pronounced effect on MED8A growth (Figure 6b). A comparable reduction in proliferative capacity was achieved with knockdown of MYC. Conversely, the medulloblastoma cell line ONS76 exhibits neither *MYC* amplification, nor a detectable PVT1-MYC fusion gene and knockdown of miR-1204 had no effect in this line (Figure 6c).

PVT1 has been reported previously in fusion transcripts with a number of partners[30,32,33]. The most prevalent form of the PVT1-MYC fusion in Group 3 tumours lacks the first, non-coding exon of MYC, similar to forms of MYC that have been described in Burkitt's lymphoma[34] (Figure 5a, d). The *PVT1* promoter contains two non-canonical E-boxes and

can be activated by MYC[31]. This suggests a positive feedback model where MYC can reinforce its own expression from the *PVT1* promoter in PVT1-MYC fusion(+) tumours. Indeed, knockdown of MYC alone in MED8A cells resulted in diminished expression of both MYC and miR-1204, suggesting MYC may positively regulate PVT1 (i.e. miR-1204) expression in medulloblastoma cells (Supplementary Figure 41).

Discussion

Medulloblastomas have few SNVs as compared to many adult epithelial malignancies[11], while SCNAs appear to be quite common. Medulloblastoma is a heterogeneous disease[7], there-by requiring large cohorts to detect subgroup specific events. Through the accumulation of >1200 medulloblastomas in MAGIC, we have identified novel and significant SCNAs. Many of the significant SCNAs are subgroup restricted, highly supporting their role as driver events in their respective subgroups.

Expression of SYNPHILIN-1 in neuronal cells results in decreased cell doubling time[35], decreased caspase-3 activation[36], decreased TP53 transcriptional activity and mRNA levels, and decreased apoptosis[37]. SYNPHILIN-1 is ubiquitinated by PARKIN, which is encoded by the hereditary Parkinson's disease gene *PARK2*[24], a candidate tumour suppressor gene[38]. While patients with Parkinson's disease have an overall decreased risk of cancer, they may have an increased incidence of brain tumours[39,40]. As tandem duplications of *SNCAIP* are highly recurrent, stereotypical, subgroup restricted, affect only a single gene, and as *SNCAIP*-duplicated tumours have few if any other SCNAs, *SNCAIP* is a probable driver gene, and merits investigation as a target for therapy of Group 4α. Similarly, *PVT1* fusion genes are highly recurrent, restricted to Group 3, arise through a chromothripsis-like process, and are the first recurrent translocation reported in medulloblastoma.

We identify a number of highly targetable, recurrent, subgroup-specific SCNAs that could form the basis for future clinical trials (i.e. PI3K signaling in SHH, TGFβ signaling in Group 3, and NF-κB signaling in Group 4). Activation of these pathways through alternative, currently unknown genetic and epigenetic events could increase the percentage of patients amenable to targeted therapy. We also identify a number of highly 'druggable' events that occur in a minority of cases. The co-operative, global approach of the MAGIC consortium has allowed us to overcome the barrier of intertumoural heterogeneity in an uncommon pediatric tumour, and to identify the relevant and targetable SCNAs for the affected children.

Methods Summary

All patient samples were obtained with consent as outlined by individual institutional review boards. Genomic DNA was prepared, processed, and hybridized to Affymetrix SNP6 arrays according to manufacturer's instructions. Raw copy number estimates were obtained in dChip, followed by CBS segmentation in R. SCNAs were identified using GISTIC2[13]. Driver genes within SCNAs were inferred by integrating matched expressions, literature evidence, and other datasets. Pathway enrichment of SCNAs was analyzed with g:Profiler and visualized in Cytoscape by enrichment mapping. FISH was performed as described previously[8,10]. Medulloblastoma subgroup was assigned using a custom nanoString CodeSet as described[12]. Tandem duplication of *SNCAIP* was confirmed by paired-end mapping as previously reported[28]. RNA was extracted, processed and hybridized to Affymetrix Gene 1.1 ST Arrays as recommended by the manufacturer. Consensus NMF clustering was performed in GenePattern. Gene fusions were identified from RNASeq data using Trans-ABySS. Medulloblastoma cell lines were maintained as described[10]. Proliferation assays

were performed with the Promega CellTiter 96 Assay. Additional methods are detailed in full in Supplementary Methods available online at Nature.com.

Supplementary Material

Refer to Web version on PubMed Central for supplementary material.

Acknowledgments

MDT is the recipient of a CIHR Clinician-Scientist Phase II award, and was formerly a Sontag Distinguished Scholar with funds from the Sontag Foundation. Funding is acknowledged from the Pediatric Brain Tumour Foundation (MDT and JTR), and the National Institutes of Health (CA159859 to MDT, RWR, and BW), Genome Canada, Genome BC, Terry Fox Research Institute, Ontario Institute for Cancer Research, Pediatric Oncology Group Ontario, Funds from 'The Family of Kathleen Lorette' and the Clark H. Smith Brain Tumour Centre, Montreal Children's Hospital Foundation, Hospital for Sick Children: Sonia and Arthur Labatt Brain Tumour Research Centre, Chief of Research Fund, Cancer Genetics Program, Garron Family Cancer Centre, B.R.A.I.N. Child, CIHR (grant # ATE-110814); the University of Toronto McLaughlin Centre, CIHR Institute of Cancer Research (grant # AT1 – 112286) and C17 through the Advancing Technology Innovation through Discovery competition (Project Title: The Canadian Pediatric Cancer Genome Consortium: Translating next-generation sequencing technologies into improved therapies for high-risk childhood cancer). Canada's Michael Smith Genome Sciences Centre is supported by the BC Cancer Foundation. JR is supported by The Children's Discovery Institute. PAN was supported by a Restracomp Fellowship (Hospital for Sick Children) and is currently a Roman-Herzog Postdoctoral Fellow (Hertie Foundation). Salary support for LG was provided by the Ontario Institute for Cancer Research through funding provided by the Government of Ontario. EVGM is supported by NIH grants CA86335, CA116804, CA138292, NCI contracts 28XS100 and 29XS193, the Southeastern Brain Tumour Foundation, and the Brain Tumour Foundation for Children. This study includes samples provided by the UK Children's Cancer and Leukaemia Group (CCLG) as part of CCLG-approved biological study BS-2007-04. JK and SP were supported by a grant from the German Cancer Aid (109252). We thank Dr. Chao Lu, Kozue Otaka, and The Centre for Applied Genomics for excellent technical assistance. We thank Narra S Devi and Zhaobin Zhang for excellent technical assistance. We thank Dominik Stoll for expert project management, Susan Archer for technical writing, and Paul Paroutis for artwork. The MAGIC project is part of the International Cancer Genome Consortium.

References

1. Gajjar A, et al. Risk-adapted craniospinal radiotherapy followed by high-dose chemotherapy and stem-cell rescue in children with newly diagnosed medulloblastoma (St Jude Medulloblastoma-96): long-term results from a prospective, multicentre trial. Lancet Oncol. 2006; 7:813–820. [PubMed: 17012043]
2. Mabbott DJ, et al. Serial evaluation of academic and behavioral outcome after treatment with cranial radiation in childhood. J Clin Oncol. 2005; 23:2256–2263. [PubMed: 15800316]
3. Cho YJ, et al. Integrative genomic analysis of medulloblastoma identifies a molecular subgroup that drives poor clinical outcome. J Clin Oncol. 2011; 29:1424–1430. [PubMed: 21098324]
4. Northcott PA, et al. Medulloblastoma comprises four distinct molecular variants. J Clin Oncol. 2011; 29:1408–1414. [PubMed: 20823417]
5. Remke M, et al. FSTL5 is a marker of poor prognosis in non-WNT/non-SHH medulloblastoma. J Clin Oncol. 2011; 29:3852–3861. [PubMed: 21911727]
6. Northcott PA, Korshunov A, Pfister SM, Taylor MD. The clinical implications of medulloblastoma subgroups. Nat Rev Neurol. 2012
7. Taylor MD, et al. Molecular subgroups of medulloblastoma: the current consensus. Acta neuropathologica. 2011
8. Northcott PA, et al. Pediatric and adult sonic hedgehog medulloblastomas are clinically and molecularly distinct. Acta Neuropathol. 2011; 122:231–240. [PubMed: 21681522]
9. Rudin CM, et al. Treatment of medulloblastoma with hedgehog pathway inhibitor GDC-0449. The New England journal of medicine. 2009; 361:1173–1178. [PubMed: 19726761]
10. Northcott PA, et al. Multiple recurrent genetic events converge on control of histone lysine methylation in medulloblastoma. Nat Genet. 2009; 41:465–472. [PubMed: 19270706]
11. Parsons DW, et al. The genetic landscape of the childhood cancer medulloblastoma. Science. 2011; 331:435–439. [PubMed: 21163964]

12. Northcott PA, et al. Rapid, reliable, and reproducible molecular sub-grouping of clinical medulloblastoma samples. Acta Neuropathol. 2012; 123:615–626. [PubMed: 22057785]
13. Mermel CH, et al. GISTIC2.0 facilitates sensitive and confident localization of the targets of focal somatic copy-number alteration in human cancers. Genome Biol. 2011; 12:R41. [PubMed: 21527027]
14. Buonamici S, et al. Interfering with resistance to smoothened antagonists by inhibition of the PI3K pathway in medulloblastoma. Science translational medicine. 2010; 2:51ra70.
15. Yauch RL, et al. Smoothened mutation confers resistance to a Hedgehog pathway inhibitor in medulloblastoma. Science. 2009; 326:572–574. [PubMed: 19726788]
16. Adamson DC, et al. OTX2 is critical for the maintenance and progression of Shh-independent medulloblastomas. Cancer Res. 2010; 70:181–191. [PubMed: 20028867]
17. Jia S, Wu D, Xing C, Meng A. Smad2/3 activities are required for induction and patterning of the neuroectoderm in zebrafish. Developmental biology. 2009; 333:273–284. [PubMed: 19580801]
18. Bizet AA, et al. The TGF-beta co-receptor, CD109, promotes internalization and degradation of TGF-beta receptors. Biochimica et biophysica acta. 2011; 1813:742–753. [PubMed: 21295082]
19. Wang T, Donahoe PK, Zervos AS. Specific interaction of type I receptors of the TGF-beta family with the immunophilin FKBP-12. Science. 1994; 265:674–676. [PubMed: 7518616]
20. Parks WT, et al. Sorting nexin 6, a novel SNX, interacts with the transforming growth factor-beta family of receptor serine-threonine kinases. The Journal of biological chemistry. 2001; 276:19332–19339. [PubMed: 11279102]
21. Bredel M, et al. NFKBIA deletion in glioblastomas. The New England journal of medicine. 2011; 364:627–637. [PubMed: 21175304]
22. Xiao N, et al. Ubiquitin-specific protease 4 (USP4) targets TRAF2 and TRAF6 for deubiquitination and inhibits TNFalpha-induced cancer cell migration. Biochem J. 2012; 441:979–986. [PubMed: 22029577]
23. Engelender S, et al. Synphilin-1 associates with alpha-synuclein and promotes the formation of cytosolic inclusions. Nature genetics. 1999; 22:110–114. [PubMed: 10319874]
24. Chung KK, et al. Parkin ubiquitinates the alpha-synuclein-interacting protein, synphilin-1: implications for Lewy-body formation in Parkinson disease. Nature medicine. 2001; 7:1144–1150.
25. Marx FP, et al. Identification and functional characterization of a novel R621C mutation in the synphilin-1 gene in Parkinson's disease. Human molecular genetics. 2003; 12:1223–1231. [PubMed: 12761037]
26. Beroukhim R, et al. The landscape of somatic copy-number alteration across human cancers. Nature. 2010; 463:899–905. 10.1038/nature08822. [PubMed: 20164920]
27. Barretina J, et al. The Cancer Cell Line Encyclopedia enables predictive modelling of anticancer drug sensitivity. Nature. 2012; 483:603–607. 10.1038/nature11003. [PubMed: 22460905]
28. Rausch T, et al. Genome sequencing of pediatric medulloblastoma links catastrophic DNA rearrangements with TP53 mutations. Cell. 2012; 148:59–71. [PubMed: 22265402]
29. Stephens PJ, et al. Massive genomic rearrangement acquired in a single catastrophic event during cancer development. Cell. 2011; 144:27–40. [PubMed: 21215367]
30. Shtivelman E, Bishop JM. The PVT gene frequently amplifies with MYC in tumor cells. Molecular and cellular biology. 1989; 9:1148–1154. [PubMed: 2725491]
31. Carramusa L, et al. The PVT-1 oncogene is a Myc protein target that is overexpressed in transformed cells. Journal of cellular physiology. 2007; 213:511–518. [PubMed: 17503467]
32. Shtivelman E, Bishop JM. Effects of translocations on transcription from PVT. Molecular and cellular biology. 1990; 10:1835–1839. [PubMed: 2181290]
33. Pleasance ED, et al. A small-cell lung cancer genome with complex signatures of tobacco exposure. Nature. 2010; 463:184–190. [PubMed: 20016488]
34. Hann SR, King MW, Bentley DL, Anderson CW, Eisenman RN. A non-AUG translational initiation in c-myc exon 1 generates an N-terminally distinct protein whose synthesis is disrupted in Burkitt's lymphomas. Cell. 1988; 52:185–195. [PubMed: 3277717]
35. Li X, et al. Synphilin-1 exhibits trophic and protective effects against Rotenone toxicity. Neuroscience. 2010; 165:455–462. [PubMed: 19857556]

36. Smith WW, et al. Synphilin-1 attenuates neuronal degeneration in the A53T alpha-synuclein transgenic mouse model. Human molecular genetics. 2010; 19:2087–2098. [PubMed: 20185556]

37. Giaime E, et al. Caspase-3-derived C-terminal product of synphilin-1 displays antiapoptotic function via modulation of the p53-dependent cell death pathway. The Journal of biological chemistry. 2006; 281:11515–11522. [PubMed: 16495229]

38. Veeriah S, et al. Somatic mutations of the Parkinson's disease-associated gene PARK2 in glioblastoma and other human malignancies. Nature genetics. 2010; 42:77–82. [PubMed: 19946270]

39. Olsen JH, et al. Atypical cancer pattern in patients with Parkinson's disease. British journal of cancer. 2005; 92:201–205. [PubMed: 15583688]

40. Moller H, Mellemkjaer L, McLaughlin JK, Olsen JH. Occurrence of different cancers in patients with Parkinson's disease. Bmj. 1995; 310:1500–1501. [PubMed: 7787596]

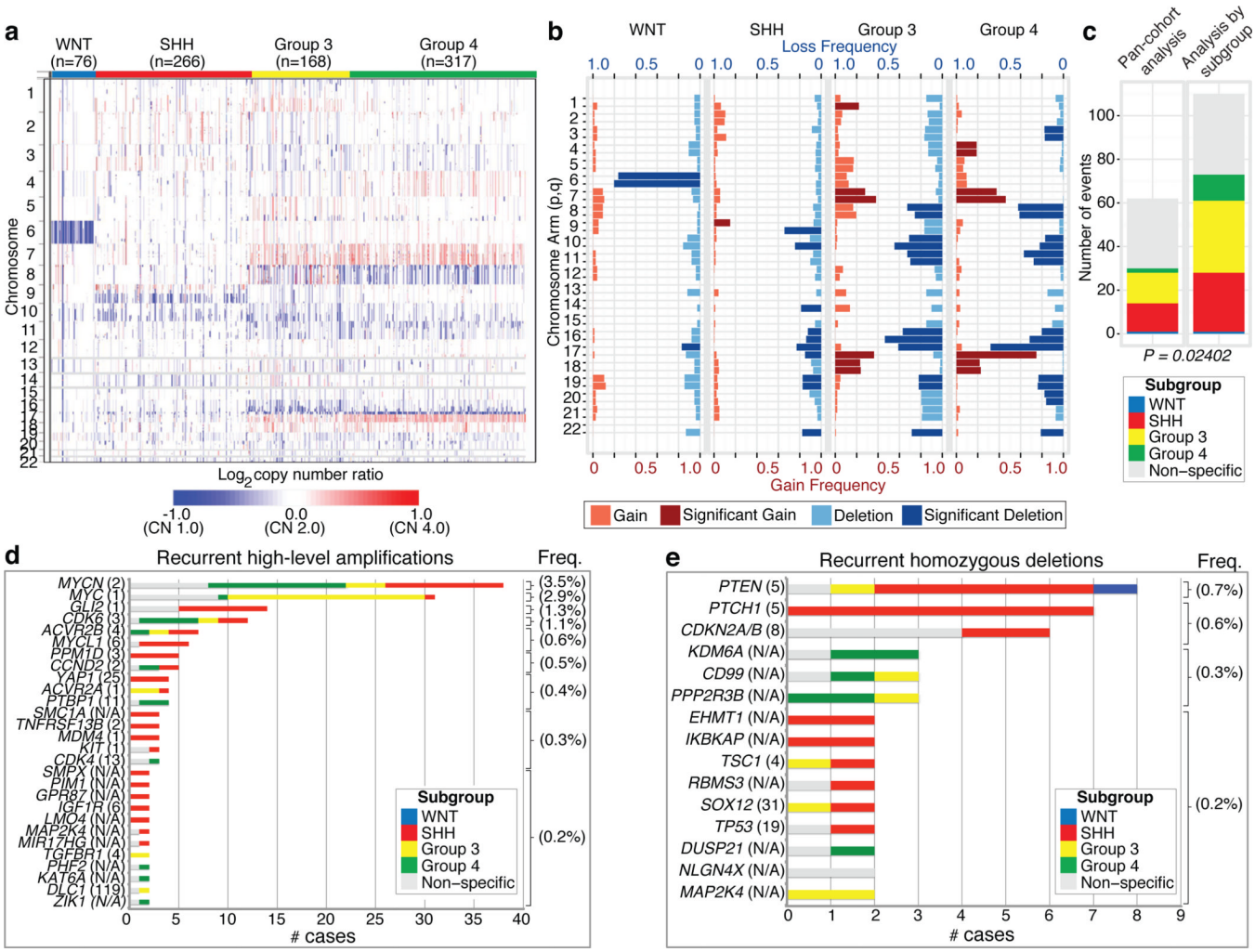

Figure 1. Genomic heterogeneity of medulloblastoma subgroups

a, The medulloblastoma genome classified by subgroup. **b,** Frequency and significance (*q*-value≤ 0.1) of broad cytogenetic events across medulloblastoma subgroups. **c,** Significant regions of focal SCNA identified by GISTIC2 in either pan-cohort or subgroup-specific analyses. **d, e,** Recurrent high-level amplifications (**d**; segmented CN≥5) and homozygous deletions (**e**; segmented CN≤0.7) in medulloblastoma. The number of genes mapping to the GISTIC2 peak region (where applicable) is listed in brackets after the suspected driver gene, as is the frequency of each event.

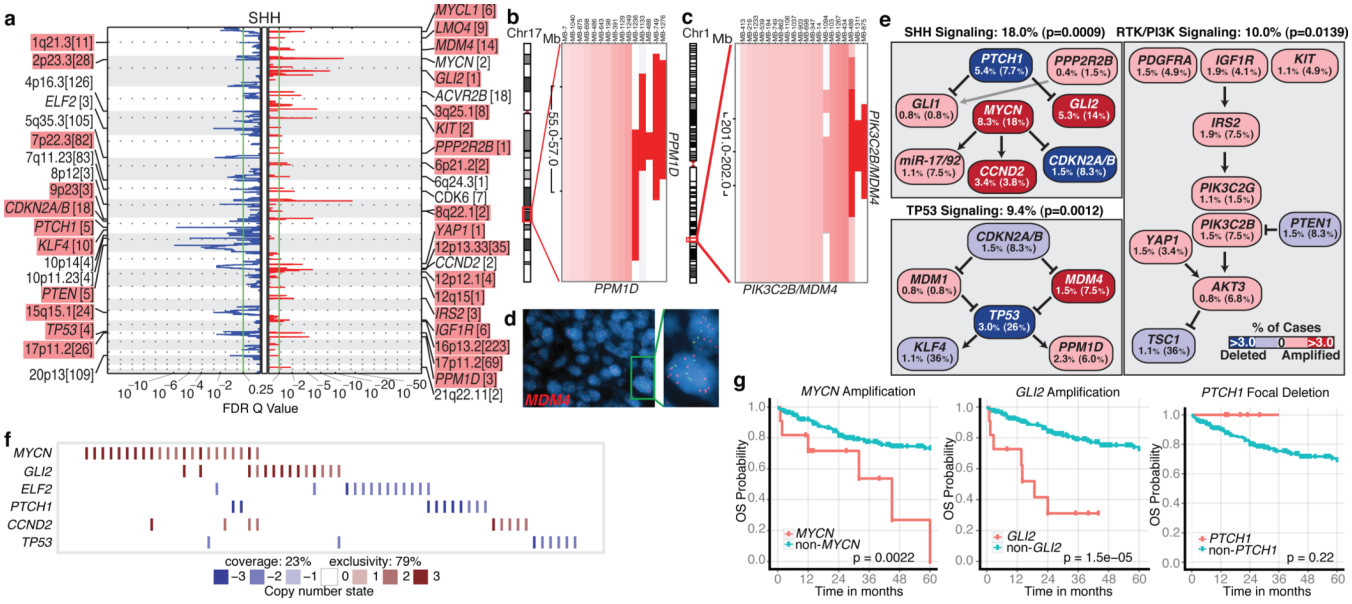

Figure 2. Genomic alterations affect core signaling pathways in SHH medulloblastoma

a, GISTIC2 significance plot of amplifications (red) and deletions (blue) observed in SHH. The number of genes mapping to each significant region are included in brackets and regions enriched in SHH are shaded red. **b, c,** Recurrent amplifications of *PPM1D* (**b**) and *PIK3C2B*/*MDM4* (**c**) are restricted to SHH. **d,** FISH validation of *MDM4* amplification. **e,** SHH signaling, TP53 signaling, and RTK/PI3K signaling represent the core pathways genomically targeted in SHH. P-values indicate the prevalence with which the respective pathway is targeted in SHH *vs.* non-SHH cases (Fisher's exact test). Frequencies of focal and broad (parentheses) SCNAs are listed. **f,** Mutual exclusivity analysis of focal SCNAs in SHH. **g,** Clinical implications of SCNAs affecting *MYCN, GLI2, or PTCH1* in SHH (log-rank tests).

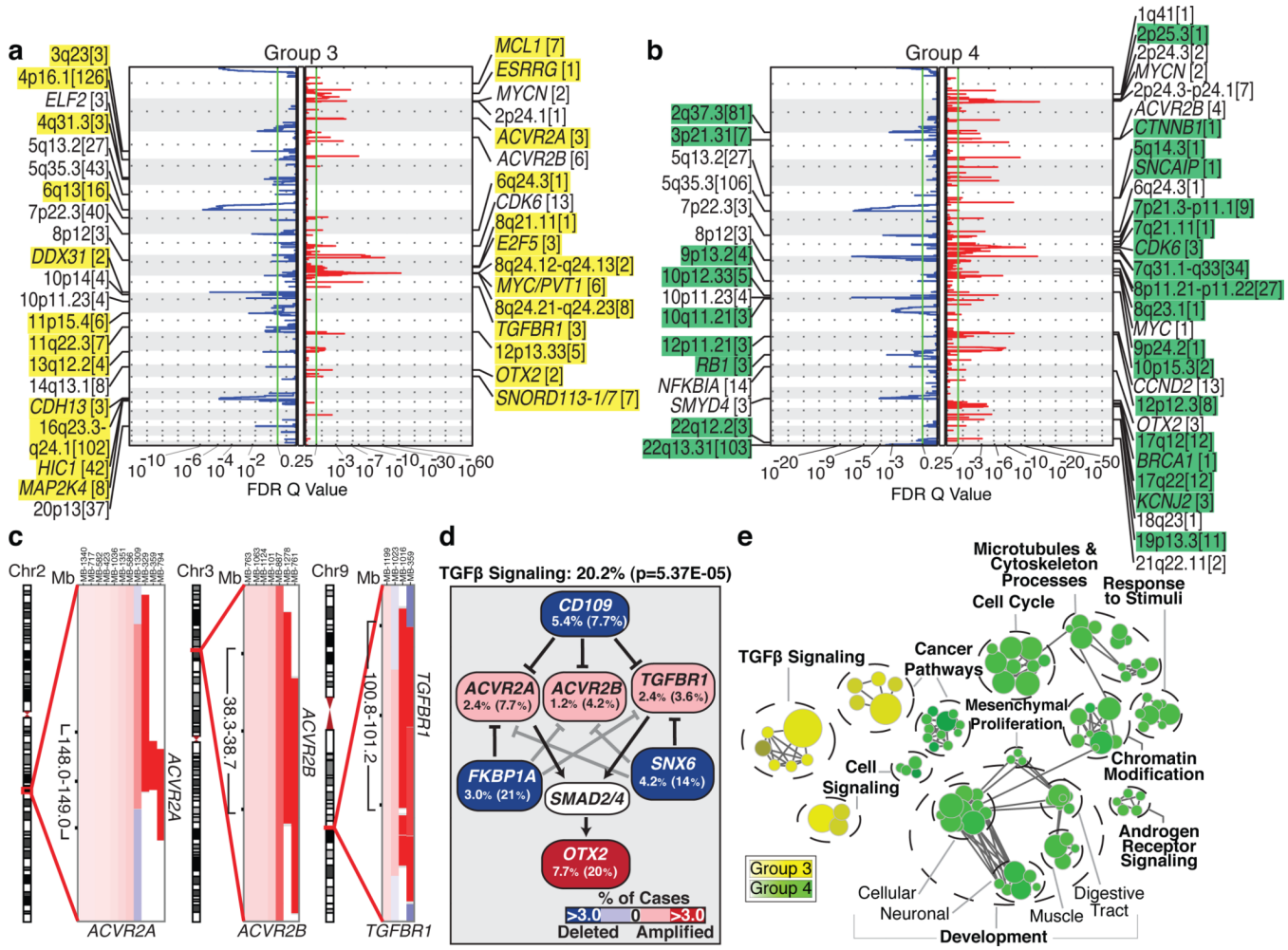

Figure 3. The genomic landscape of Group 3 and Group 4 medulloblastoma

a, b, GISTIC2 plots depicting significant SCNAs in Group 3 (**a**) and Group 4 (**b**) with subgroup-enriched regions shaded in yellow and green, respectively. **c,** Recurrent amplifications targeting type II (*ACVR2A* and *ACVR2B*) and type I (*TGFBR1*) activin receptors in Group 3. **d,** Recurrent SCNAs affecting the TGFβ pathway in Group 3 (P=5.73E-05, Fisher's exact test). Frequencies of focal and broad (parentheses) SCNAs are listed. **e,** Enrichment plot of gene sets affected by SCNAs in Group 3 *vs.* Group 4.

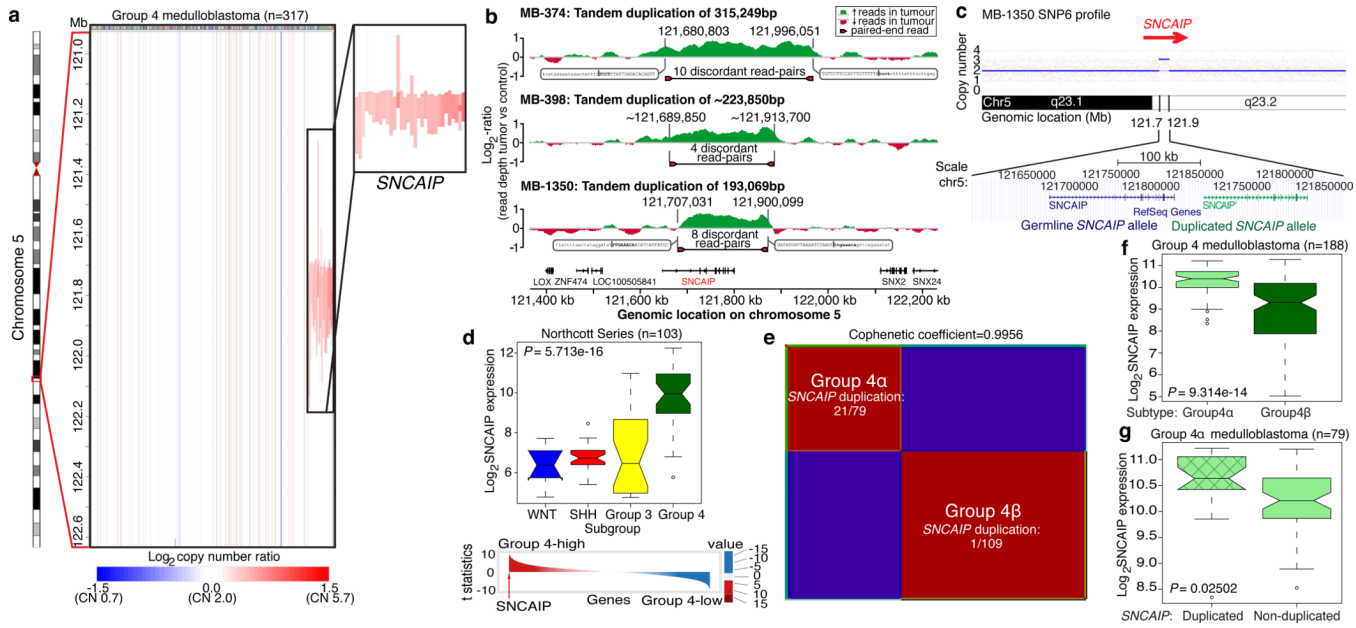

Figure 4. Tandem duplication of *SNCAIP* defines a novel subtype of Group 4

a, Highly recurrent, focal, single copy gain of *SNCAIP* in Group 4. **b,** Paired-end mapping verifies recurrent tandem duplication of *SNCAIP* in Group 4. **c,** Schematic representation of *SNCAIP* tandem duplication. **d,** *SNCAIP* is a Group 4 signature gene. *Upper panel.* SNCAIP expression across subgroups in a published series of 103 primary medulloblastomas. *Lower panel.* SNCAIP ranks among the top 1% (rank=39/16,758) of highly expressed genes in Group 4. **e,** NMF consensus clustering of 188 expression-profiled Group 4s supports two transcriptionally distinct subtypes designated 4α and 4β (Cophenetic coefficient=0.9956). 21/22 *SNCAIP* duplicated cases belong to Group 4α (P=3.12E-08, Fisher's exact test). **f,** SNCAIP expression is significantly elevated in Group 4α *vs.* 4β (P=9.31E-14, Mann-Whitney test). **g,** Group 4α cases harboring *SNCAIP* duplication exhibit a ~1.5-fold increase in SNCAIP expression.

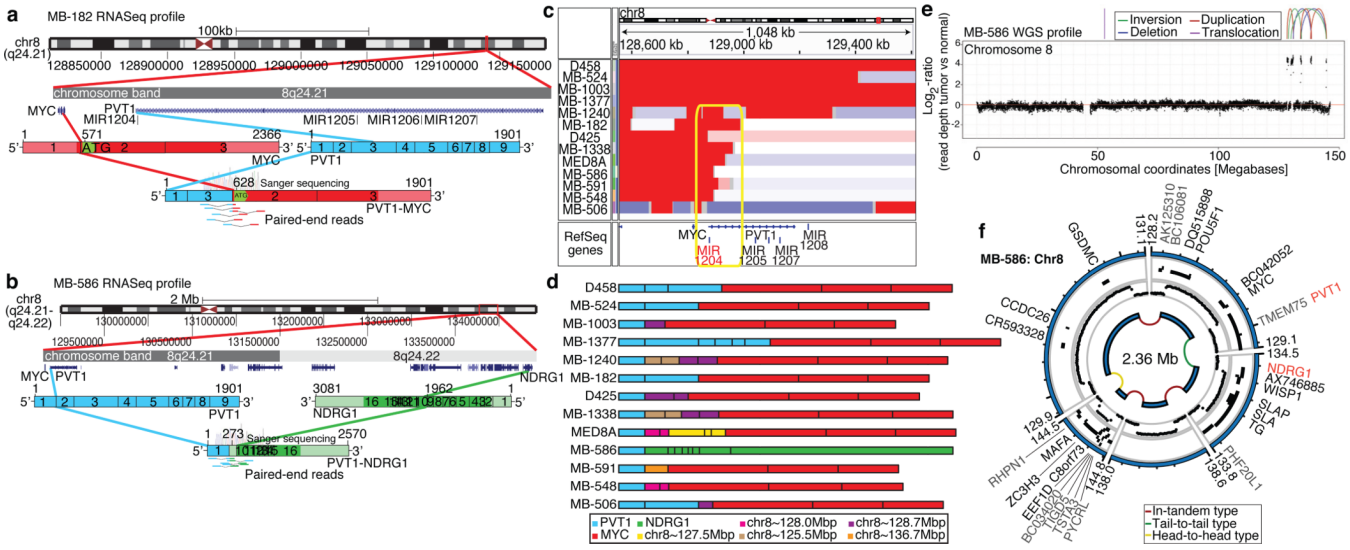

Figure 5. Identification of frequent PVT1-MYC fusion genes in Group 3

a, b, RNASeq identifies multiple fusion transcripts driven by PVT1 in Group 3. Schematics depict the structures of verified PVT1-MYC (**b**) and PVT1-NDRG1 (**c**) fusion genes. **c,** Heatmap of the *MYC/PVT1* locus showing a subset of 13 *MYC*-amplified Group 3 cases subsequently verified to exhibit PVT1 gene fusions (shown in **d**). Yellow box highlights the common breakpoint affecting the first exon/intron of *PVT1*, including miR-1204. **d,** Summary of PVT1 fusion transcripts identified in Group 3. **e, f,** WGS confirms complex patterns of rearrangement on chr8q24 in PVT1 fusion(+) Group 3.

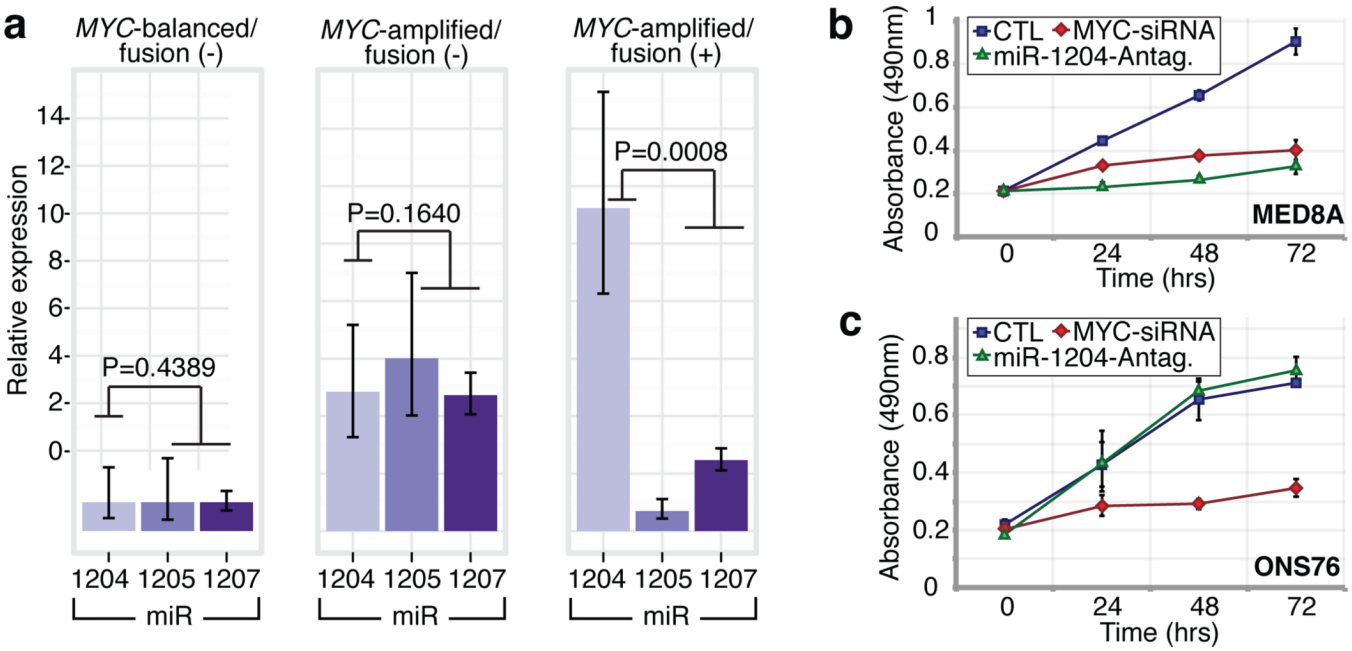

Figure 6. Functional synergy between miR-1204 and MYC secondary to PVT1-MYC fusion

a, qRT-PCR of PVT1-encoded microRNAs confirms up-regulation of miR-1204 in PVT1-MYC fusion(+) Group 3s: *MYC*-balanced/fusion(−), n=4; *MYC*-amplified/fusion(−), n=6; *MYC*-amplified/fusion(+), n=8. Error bars represent standard error of the mean (SEM) and reflect variability among samples. **b, c** Knockdown of miR-1204 attenuates the proliferative capacity of PVT1-MYC fusion(+) MED8A medulloblastoma cells (**b**) but has no effect on fusion(−) ONS76 cells (**c**). Error bars represent the standard deviation (SD) of triplicate experiments.